Bulk Heterojunction Organic Solar Cells Based on Hydrogen-Bonding Functionalized Organic Photoactive Materials

Daken J. Starkenburg,[1] Asmerom O. Weldeab,[2] Danielle E. Fagnani,[2] Lei Li,[2]
Zhengtao Xu,[1] Xiaoyang Yan,[2] Michael J. Sexton,[1] Davita L. Watkins,[2]
Ronald K. Castellano,[2] and Jiangeng Xue[1]

[1] Department of Materials Science and Engineering

[2] Department of Chemistry

University of Florida, Gainesville, FL 32611

Final Scientific/Technical Report

Project Title:	Single-Junction Organic Solar Cells with >15% Efficiency
Project Period:	05/01/16 – 10/30/17
Recipient:	University of Florida
Award Number:	DE-EE0007362

Principal Investigator: Jiangeng Xue
Professor of Materials Science and Engineering
Phone: 352-846-3775
Fax: 352-846-3355
Email: jxue@mse.ufl.edu

Acknowledgement:
"This material is based upon work supported by the Department of Energy under Award Number(s) DE-EE0007362*"*

Executive Summary

Organic solar cells have the potential to offer low-cost solar energy conversion due to low material costs and compatibility with low-temperature and high throughput manufacturing processes. This project aims to further improve the efficiency of organic solar cells by applying a previously demonstrated molecular self-assembly approach to longer-wavelength light-absorbing organic materials. The team at the University of Florida designed and synthesized a series of low-bandgap organic semiconductors with functional hydrogen-bonding groups, studied their assembly characteristics and optoelectronic properties in solid-state thin film, and fabricated organic solar cells using solution processing. These new organic materials absorb light up 800 nm wavelength, and provide a maximum open-circuit voltage of 1.05 V in the resulted solar cells. The results further confirmed the effectiveness in this approach to guide the assembly of organic semiconductors in thin films to yield higher photovoltaic performance for solar energy conversion. Through this project, we have gained important understanding on designing, synthesizing, and processing organic semiconductors that contain appropriately functionalized groups to control the morphology of the organic photoactive layer in solar cells. Such fundamental knowledge could be used to further develop new functional organic materials to achieve higher photovoltaic performance, and contribute to the eventual commercialization of the organic solar cell technology.

Project Objectives

The goal of this one-year SIPS project is to increase the power conversion efficiency (PCE) of single-junction organic solar cells by >50%, from the current ~10% to >15%, by leveraging a recent innovation by the Project Team in controlling the three-dimensional organization and assembly of organic photovoltaic materials using tailored hydrogen bonding (HB). Performance of existing organic solar cells using the donor-acceptor heterojunction structure to separate photogenerated charge carriers strongly depend on the three-dimensional morphological structure of the heterojunction photoactive layer. While the community has gained tremendous knowledge in recent years to control the energetics at the donor-acceptor heterojunction and the light absorption characteristics of the constituent materials through proper chemical structure design/modification, the complex interactions among the organic molecules or polymers and the complex thermodynamics and kinetics in material processing often result in non-ideal and unpredictable active layer morphologies that yield non-optimal charge generation and transport characteristics. The hydrogen bonding (HB) mediated supramolecular self-assembly approach studied here is anticipated to generate “programmed” organic active layer morphologies that have superior charge separation and transport properties and are relatively insensitive to the chemical structure of the light absorbing units. Hence, by applying this concept to the most efficient solution-processible molecular system, a (dicyanomethylene)rhodanine-terminated oligothiophene, we expect to achieve significant improvement in both short-circuit current (~30%) and fill factor (~20%) of the solar cells, leading to an increase in the power conversion efficiency from ~10% to >15%. There are three specific objectives in this project:

- Develop new organic donor oligomers with tailored hydrogen-bonding functional groups;
- Demonstrate organic bulk heterojunction structures with optimal charge separation and transport properties using these new HB-functionalized donor materials; and
- Fabricate single-junction organic solar cells based on the new HB-functionalized donor materials to demonstrate >15% PCE.

Detailed Project Activities:

1. Hydrogen bonding mediated supramolecular assembly approach

Performance of existing organic solar cells using the donor-acceptor heterojunction structure to separate photogenerated charge carriers strongly depend on the three-dimensional morphological structure of the heterojunction photoactive layer. While the community has gained tremendous knowledge in recent years to control the energetics at the donor-acceptor heterojunction and the light absorption characteristics of the constituent materials through proper chemical structure design/modification, the complex interactions among the organic molecules or polymers and the complex thermodynamics and kinetics in material processing often result in non-ideal and unpredictable active layer morphologies that yield non-optimal charge generation and transport characteristics.

The circumvent these challenges, the research team at the University of Florida consisting of the PI Jiangeng Xue (Materials Science and Engineering) and Co-PI Ronald Castellano (Chemistry) developed a hydrogen bonding (HB) mediated supramolecular self-assembly approach to generate “programmed” organic active layer morphologies that have superior charge separation and transport properties and are relatively insensitive to the chemical structure of the light absorbing units.

As illustrated in Fig. 1, we intend to synthetically fuse a carefully chosen HB unit to conjugated organic donor (D) unit that has desired electronic and optical properties for photovoltaic functions. The in-plane H-bonding interactions among the HB units will guide the self-assembly of the HB-D complexes (the new donor oligomers) into specific topological structures (trimers as shown, or tetramers, hexamers, etc.). π-Stacking of these donor arrays in the out-of-plane direction will further organize them into vertically aligned columnar domains with small in-plane sizes (a few nm). In this way, we expect to achieve fine mixing of the donor and acceptor (e.g. fullerene) species in the in-plane directions and contiguous vertical pathways for efficient charge transport at the same time. The overall nanoscale phase-separated and percolated morphology, which is strongly dictated by the intermolecular H-bonding interactions among the HB units, is also expected to be relatively insensitive to specific donor chromophore molecular structures, thus allowing us to independently optimize the electronic structure and optical properties of the donor unit for maximum photovoltaic performance.

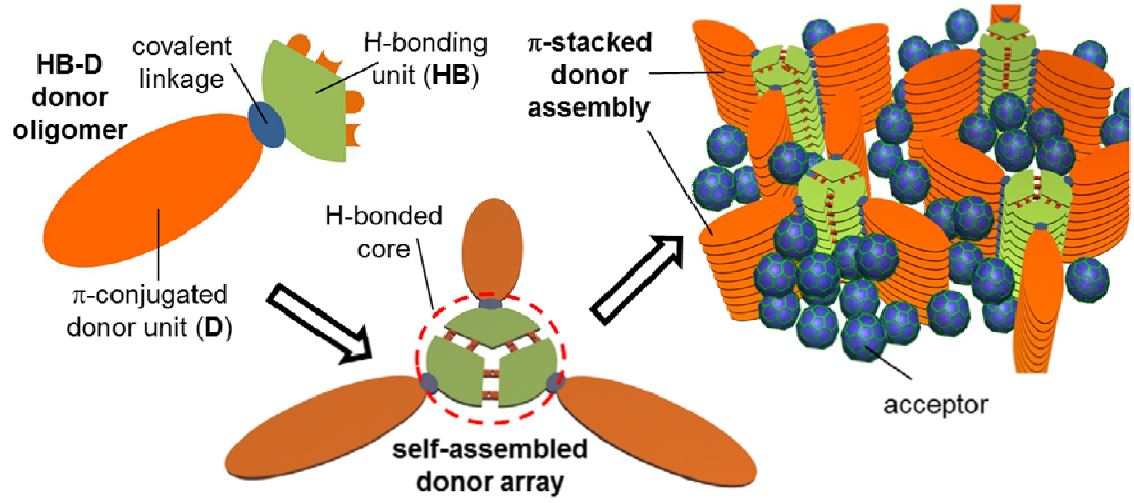

Fig. 1. Schematic illustration of the proposed HB-mediated supramolecular self-assembly approach to programmed organic bulk heterojunctions.

Previously, the research team synthesized simple quaterthiophene donors with infused phthalhydrazide (PH) HB units (see Fig. 2). The PH units organize the HB-D complexes into trimers, which were indeed observed on Au(111) surfaces using scanning tunneling microscopy.

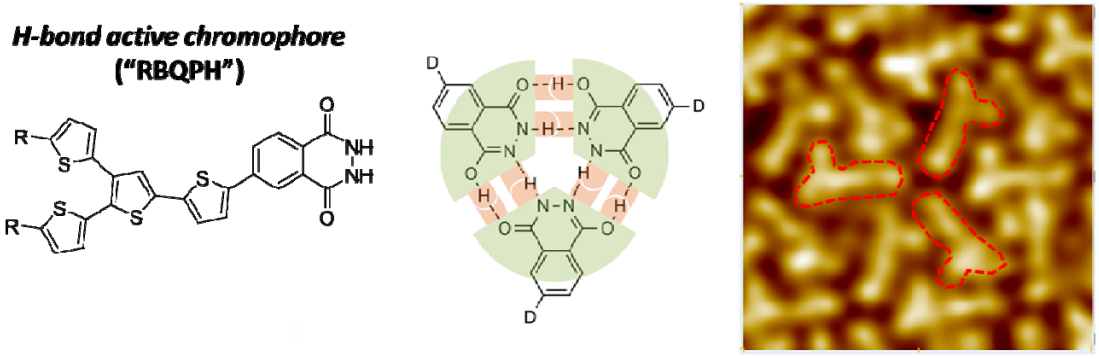

(a) (b) (c)

Fig. 2. Previously synthesized oligothiophene HB-D oligomers: (a) molecular structure, (b) schematic H-bonding among PH units, (c) scanning tunneling microscopy image showing the formation of BQPH trimers on Au(111) surface.

Fig. 3(a) shows a comparison of grazing-incidence wide-angle X-ray scattering results of vacuum-deposited, HB-D:fullerene mixed thin films for both the HB-enabled species (LQPH) and a comparator molecule (LQPME) with disabled H-bonding interactions. The X-ray scattering results clearly shows the π-π stacking direction in the HB-enabled film is preferentially in the vertical direction as we have anticipated (suggesting a face-on orientation for the HB-D oligomers), whereas the π-π stacking direction in the HB-disabled film is in the in-plane direction (suggesting an edge-on orientation for the comparator oligomers). The phase image of the LQPH:C_{60} film surface from atomic force microscopy shown in Fig. 3(b) is nearly featureless, in agreement with the anticipated in-plane fine intermixing of the donor and acceptor species. The LQPME:C_{60}

film, on the other hand, show clear phase separated structures with >20 nm domain sizes. Comparing the HB-enabled oligomers to the comparator oligomers, the resulted organic solar cells show over 50% increase in the peak external quantum efficiencies (EQEs) and overall red-shifted spectral response [see Fig. 3(c)], which lead to approximately doubling in the power conversion efficiencies (PCE). Worth mentioning is that the linear quaterthiophene (LQ) systems also show ~25% higher EQEs than the corresponding branched quaterthiophene (BQ) systems. We attribute this difference to the more planar structure of the LQ donor unit, which should facilitate the π-π stacking among the HB-D oligomers and hence improved charge transport.

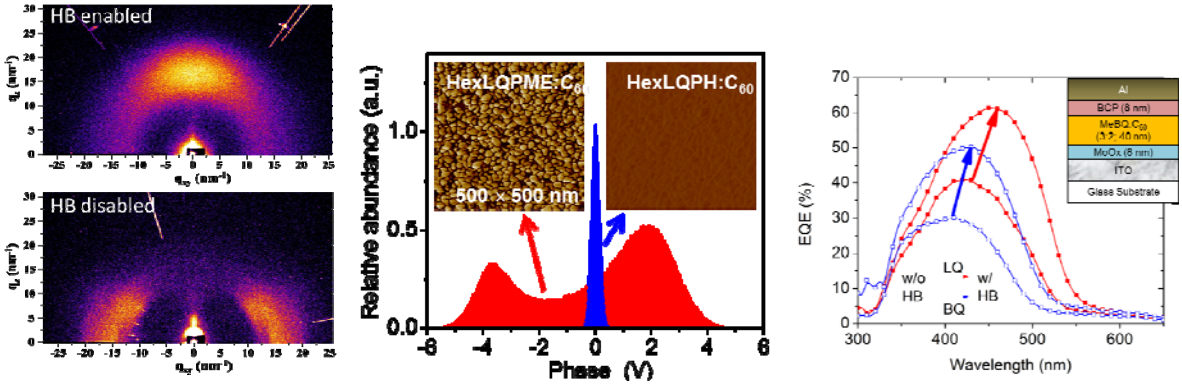

(a) (b) (c)

Fig. 3. Thin films and solar cells based on the oligothiophene HB-D oligomers as compared to comparator molecules without H-bonding activity: (a) grazing-incidence wide-angle X-ray scattering, (b) atomic-force microscopy phase image, (c) external quantum efficiency spectra of organic solar cells.

2. Design of hydrogen bonding (HB) functionalized donor oligomers

As shown in Fig. 3(c), while the previous work demonstrated the feasibility of the HB-mediated supramolecular approach, the simple quaterthiophene donor units used do not have good coverage of the solar spectrum. The absorption edge of these thiophene oligomers is in the range of 500 to 550 nm. Hence, the focus of this project is to expand this general approach to donor systems with more optimal light absorption properties, i.e., a much narrower HOMO-LUMO band gap. The donor system we chose to implement on is 2,2'-((5Z,5'Z)-5,5'-((3,3'''-dioctyl-[2,2':5',2'':5'',2'''-oligothiophene]-5,5'''-diyl)bis(methanylylidene))bis(3-(2-ethylhexyl)-4-oxothiazolidine-5,2-diylidene))dimalo nonitrile (**DRCNnT**, n = 4 to 7), which has been shown previously by others to produce 10% PCE in optimized organic solar cells.

The first step in this project is to use density-functionale theory (DFT) based calculations to examine the HOMO and LUMO energy levels (and therefore the band gap) of various HB-D oligomer designs. The HB candidates we examined include phthalhydrazide (**PH**), guanine (**G**), diaminotriazine (**DAT**), and barbiturate (**B**), which give rise to three-, four-, six- and six-fold H-bonded donor assemblies, respectively, as illustrated in Fig. 4. The corresponding HB-disabled comparator oligomers are also shown.

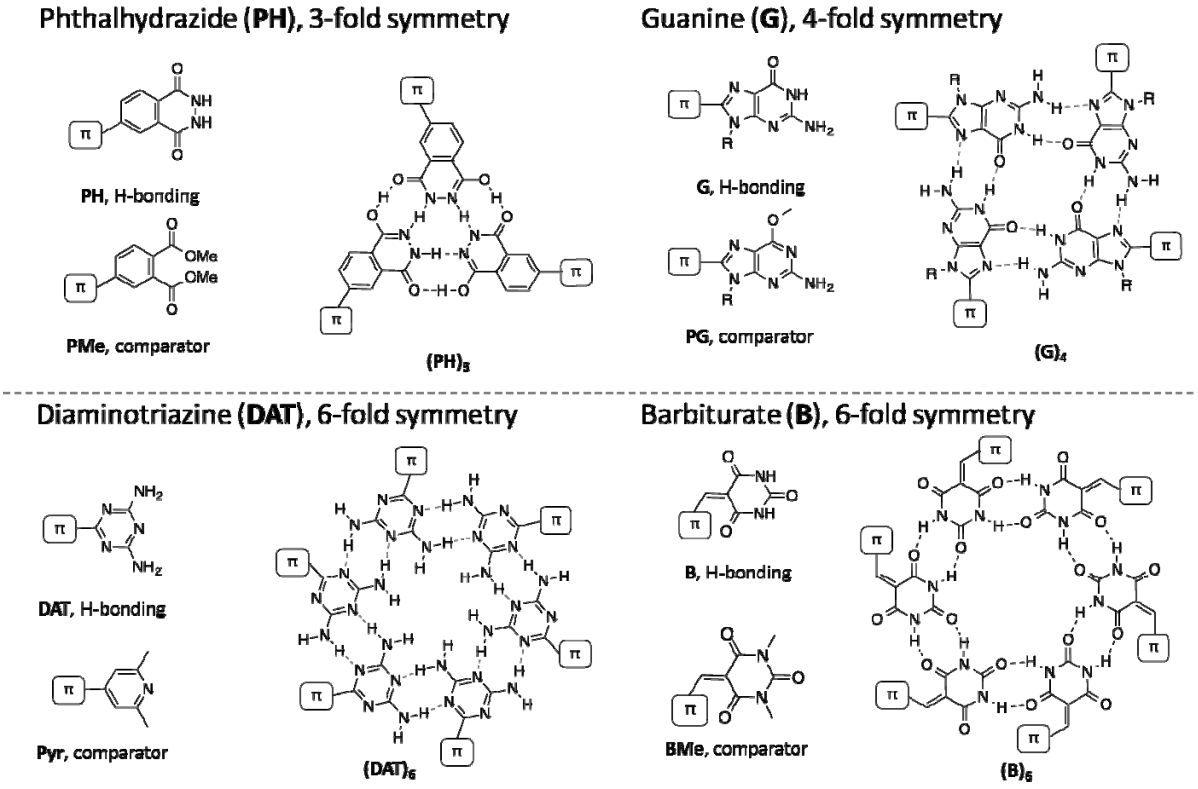

Fig. 4. Four candidate HB moieties examined in this work.

The calculated HOMO/LUMO energy levels (B3LYP/6-31+G*) of the RCNnT-HB oligomers with different HB units and varying oligothiophene length (n = 4,5,6,7) are shown in Fig. 5 along with the molecular structures. It is cautioned that these calculated energies may not accurate reflected the actual energies of these oligomers in solid-state films, due to the well-known limitation of DFT theories (which generally underestimate band gaps) and the gas-phase environment used for calculation (which overestimates band gaps compared to solid-state environment in films). Nevertheless, trends in the calculated results are still very useful for us to understand the effects of the HB unit and the oligothiophene length on the electronic behavior of the HB-D oligomers. For example, as n is increased from 4 to 7, we see a gradual rise in the HOMO level (by 0.2 to 0.3 eV) while the LUMO level remains unchanged, leading to a gradual decrease in the HOMO-LUMO gap (by 0.2 to 0.3 eV). Barbiturate appears to result in deepest lying HOMO levels (up to 5.6 eV below the vacuum level), whereas guanine appears to generate the highest lying HOMO levels. As a result, for HB-D oligomers with the same oligothiophene length, those with barbiturate have the greatest HOMO-LUMO gaps, and those with guanine have the smallest gaps, although the difference is also within 0.2 to 0.3 eV.

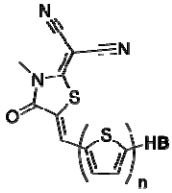

Numbers in (parentheses) are differences in neighboring energy levels:

e.g., HOMO(n) - HOMO(n-1)

HB	n	HOMO (eV)	LUMO (eV)	E_g (eV)
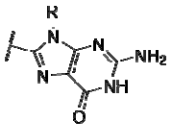	4	-5.35	-3.30	2.04
	5	-5.25 (+0.10)	-3.31 (-0.01)	1.94 (-0.11)
G	6	-5.17 (+0.08)	-3.32 (-0.01)	1.85 (-0.09)
	7	-5.11 (+0.06)	-3.33 (-0.01)	1.78 (-0.07)
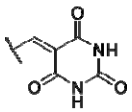	4	-5.63	-3.34	2.29
	5	-5.46 (+0.17)	-3.27 (+0.07)	2.20 (-0.09)
B	6	-	-	-
	7	-5.50	-3.48 (-0.14)	2.02 (-0.27)
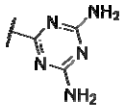	4	-5.56	-3.34	2.22
	5	-5.42 (+0.14)	-3.35 (-0.01)	2.07 (-0.15)
DAT	6	-5.31 (+0.11)	-3.35 (0.00)	1.96 (-0.11)
	7	-5.23 (+0.08)	-3.35 (0.00)	1.88 (-0.08)
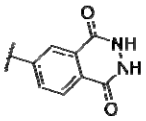	4	-5.65	-3.42	2.23
	5	-5.51 (+0.14)	-3.40 (+0.01)	2.11 (-0.12)
PH	6	-5.40 (+0.11)	-3.39 (+0.01)	2.01 (-0.10)
	7	-5.31 (+0.09)	-3.38 (+0.01)	1.93 (-0.08)

Fig. 5. Calculated HOMO/LUMO energy levels of various RCNnT-HB oligomers with different HB units and variable oligothiophene length.

3. Synthesis, purification, and characterization of HB-D oligomers

Given that the barbiturate units result in deepest lying HOMO levels, which is useful for producing high voltage output in organic solar cells, the synthetic work started with this HB unit, although subsequent work also began on PH and DAT HB units. Also we started with shorter oligothiophenes (*n* = 4,5). Fig. 6 summarizes the work progress on synthetic work on the target HB-D oligomers, along with the molecular structure of the example molecule of RCN_5T_HB. At the end of this reporting period, we have completed the synthesis, purification, and most of the basic characterization work (other than ^{13}C NMR) of both RCN_4T_B and RCN_5T_B. The corresponding PH and DAT oligomers have also been either already synthesized or in the final step of synthesis.

example: RCN_5T_HB_dg

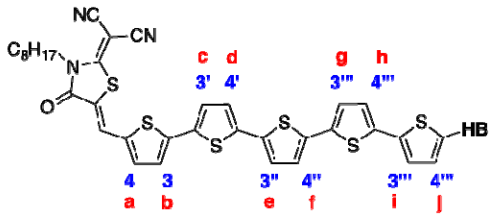

Compound	synthesis	purification	^{1}HNMR	^{13}CNMR	HRMS	UV-Vis (solution)	TGA
RCN_3T_PH	■	■	■	■	■	■	■
RCN_4T_B_df	✓	✓	✓	■	✓	✓	✓
RCN_4T_BMe_df	✓	✓	✓	✓	✓	✓	✓
RCN_5T_B_dg	✓	✓	✓	■	✓	✓	✓

✓ = complete; ■ = in progress; O= rapid completion upon purification

Fig. 6. Progress summary of synthesizing various target HB-D oligomers.

The multi-step synthetic process of obtaining the aldehyde building blocks is illustrated in Fig. 7(a). The steps of synthesizing RCN_4T_B and RCN_5T_B are shown in Figs. 7(b) and 7(c). Particularly worth mentioning is that we were able to simplify the synthetic process, and obtain both the benchmark comparator oligomer (DRCN5T) in the same reaction as RCN_5T_B oligomer by using bifunctionalized building blocks [see Fig. 7(c)]. The separation of DRCN5T and RCN_5T_B was readily achieved in chromatography columns.

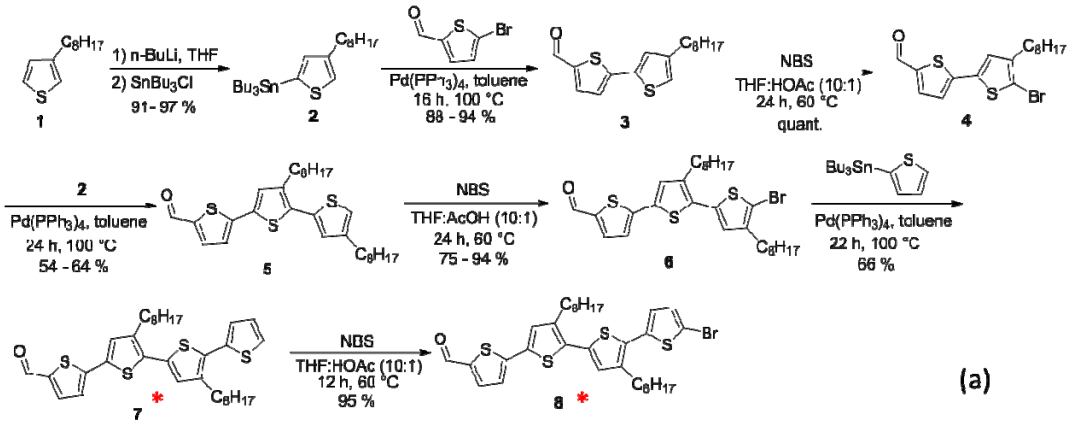

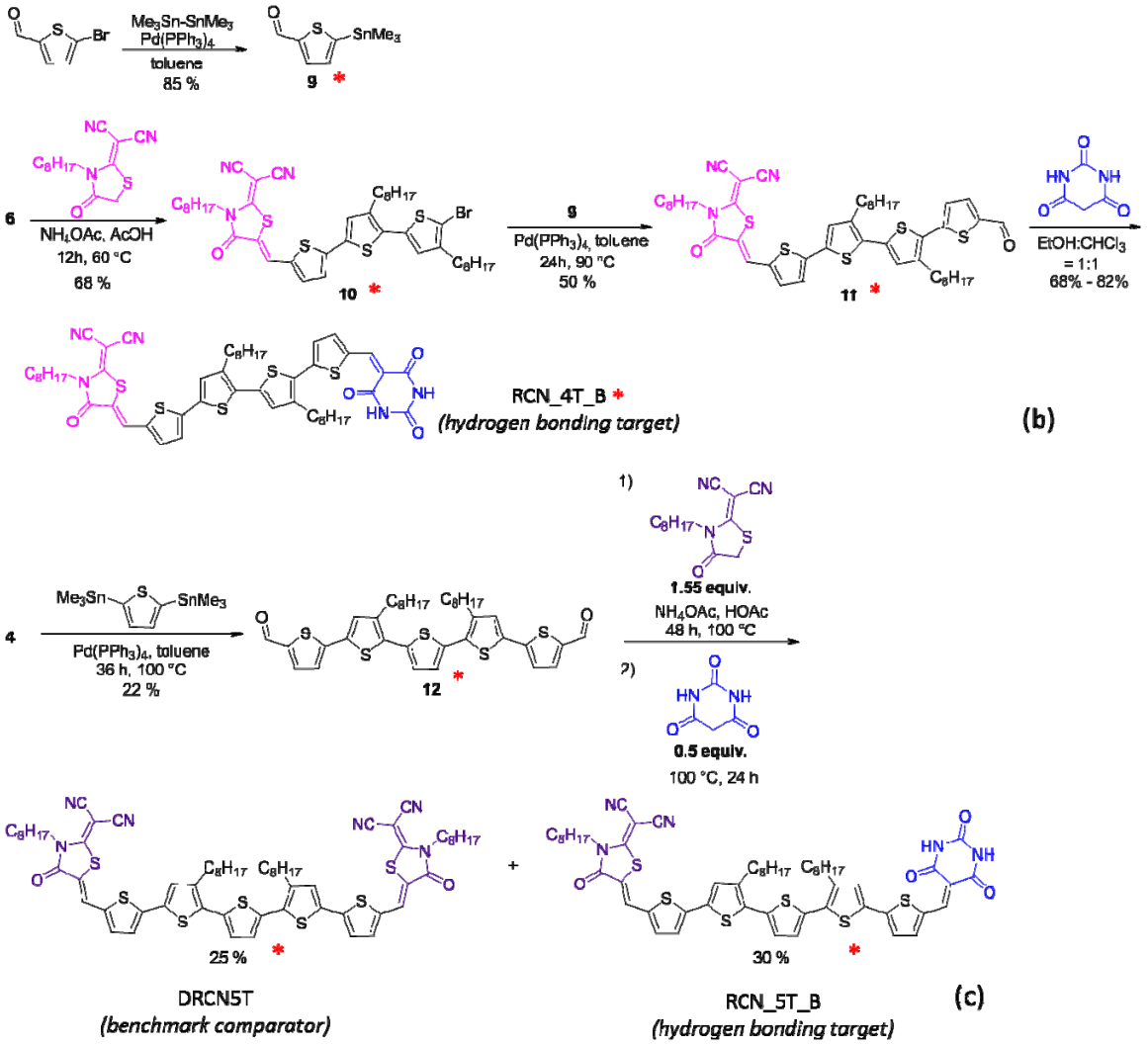

Fig. 7. Synthetic process of obtaining (a) aldehyde building blocks, (b) RCN_4T_B, and (c) RCN_5T_B (and DRCN5T comparator). The red star signs indicate new compounds.

Figure 8 shows the UV-vis-NIR absorption spectra of the target oligomers in solution. RCN_4T_B in tetrahydrofuran (THF) solvent shows peak absorption at λ_{max} = 519 nm and an absorption onset of λ_{on} = 620 nm (corresponding to a photon energy of 2.0 eV), which are shifted to λ_{max} = 554 nm and λ_{on} = 650 nm (photon energy = 1.9 eV) in chloroform ($CHCl_3$) solvent. This may be due to the incomplete solvation of this oligomer in chloroform. RCN_5T_B in chloroform show slightly red-shifted absorption as compared to the comparator DRCN5T in chloroform with λ_{max} = 551 nm vs. 538 nm and λ_{on} = 665 nm (1.86 eV) vs. 645 nm (1.92 eV). A four-fold increase in solubility for RCN_5T_B was obtained in a mixed solvent of chloroform with dichlorobenzene (DCB) and dimethylformamide (DMF); in this case, the absorption spectrum is nearly identical to that of the comparator molecule DRCN5T.

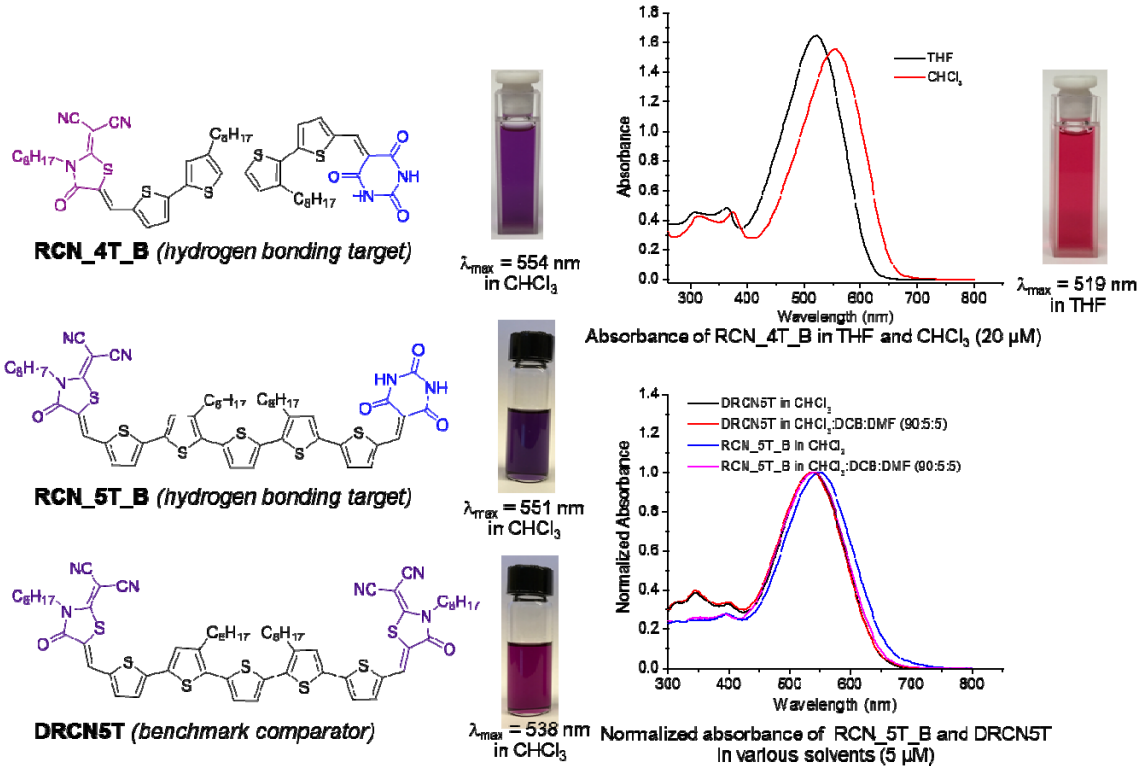

Fig. 8. UV-vis-NIR absorption spectra of target oligomers in solution.

We also used Thermogravimetric Analysis (TGA) to evaluate the thermal properties of RCN_4T_B along with the HB-inactive comparator molecular RCN_4T_BMe. As shown in Fig. 9, both materials are reasonably with 5% mass loss occurring at temperatures above 300 °C.

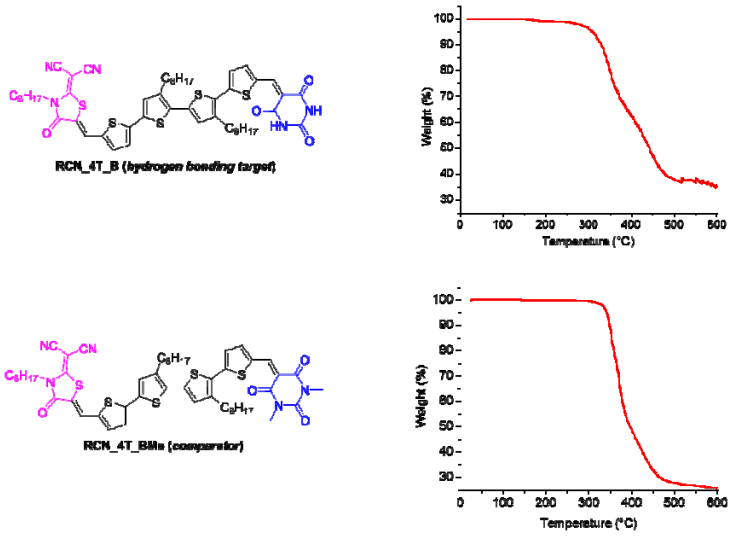

Fig. 9. TGA of RCN_4T_B (5% loss = 308°C) and RCN_4T_BMe (5% loss = 341°C)

4. Thin-film Deposition and Characterization

Given the relative large size of the oligomers, solution processing was used to prepare organic thin films. Some alkyl solubilizing chains have been included on both the oligothiophene and acceptor units. The solution processing of the target oligomers was complicated by the need to break up the intermolecular H-bonding in solution. This was evidenced by the relatively low solubility of the HB-enabled oligomers in chloroform. For example, the solubility of RCN_5T_B is ~1 mg/mL in chloroform. By including a co-solvent that may H-bond to the target oligomers, such as DMF, we were able to drastically improve the solubility of RCN_5T_B to 4 mg/mL (CF:DCB:DMF=90:5:5) to 8 mg/mL (DCB:DMF=60:40).

Using the co-solvent approach and relatively low spin-coating speed (500 to 1000 rpm), we were able to prepare 50 to 100 nm thick films of neat HB-D films or HB-D:PCBM mixed films. As shown in Fig. 10, the absorption peak of RCN_5T_B red-shifted by 30 nm from solution to thin film; a more significant red-shift, by ~100 nm to ~750 nm (photon energy = 1.65 eV), was obtained in the absorption onset of RCN_5T_B. Similar red-shifts were obtained for the comparator molecule (labeled as RCN_5T_RCN) we synthesized, although a more pronounced shoulder at ~650 nm was observed (as compared to a minor shoulder at ~680 nm for RCN_5T_B). This shoulder peak in the absorption spectra often signifies ordering in the packing of the conjugated molecules. For the mixed oligomer:$PC_{61}BM$ films, we see that the absorption features of the oligomers (both RCN_5T_B and RCN_5T_RCN) are retained. Additional features at < 450 nm also appear, which are attributed to PCBM absorption. We note that the literature report on DRCN5T (B. Kan et al., *J. Am. Chem. Soc*. **137**, 3886 (2015).) show about 50 nm further red-shifted absorption compared to our RCN_5T_RCN molecule despite the minor differences in molecular structure (mostly concerning the position and length of solubilizing chains). This issue will need to further investigated, which may be related to the fact that DRCN5T is somewhat an outlier in their entire oligothiophene series ($4 \le n \le 8$) based on the literature work.

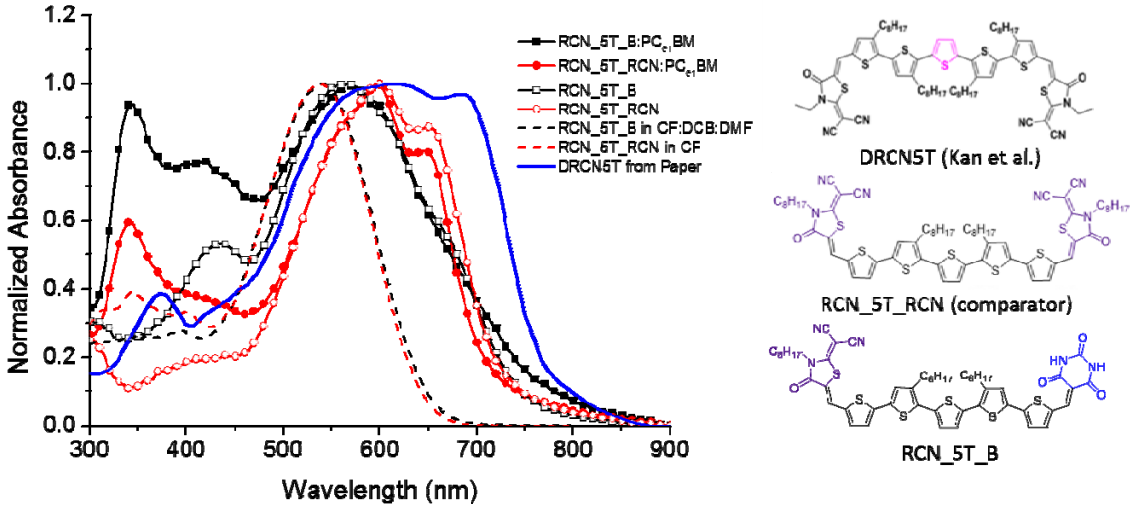

Fig. 10. UV-vis-NIR absorption spectra of RCN_5T_B and RCN_5T_RCN in solution (dashed lines) and in solid-state films (open symbols) as well as in mixed films with $PC_{61}BM$ (solid symbols). Also shown is the reference spectrum of DRCN5T from literature.

Atomic force microscopy (AFM) was used to examine the surface morphology of the HB-D oligomer:PCBM mixed films. As shown in Fig. 11, for RCN_4T_B mixed with $PC_{71}BM$, we observed that the domain sizes are relatively large, >100 nm. Further investigation is needed to clearly identify what these large domains are. But this likely suggests that the phase separation is too strong in the mixed films, which is not very desirable for bulk heterojunctions and may indicate the low miscibility between the two molecules. Suppressing phase separation between the donor and acceptor species will be an important task in the remainder period of this project. There also appears to be some influence on the domain sizes as the chlorobenzene (CB) content is varied in the THF:CB co-solvent. We further performed thermal annealing experiments on these mixed thin films. AFM studies revealed that the annealing resulted in a slight increase in the domain sizes (see Fig. 12).

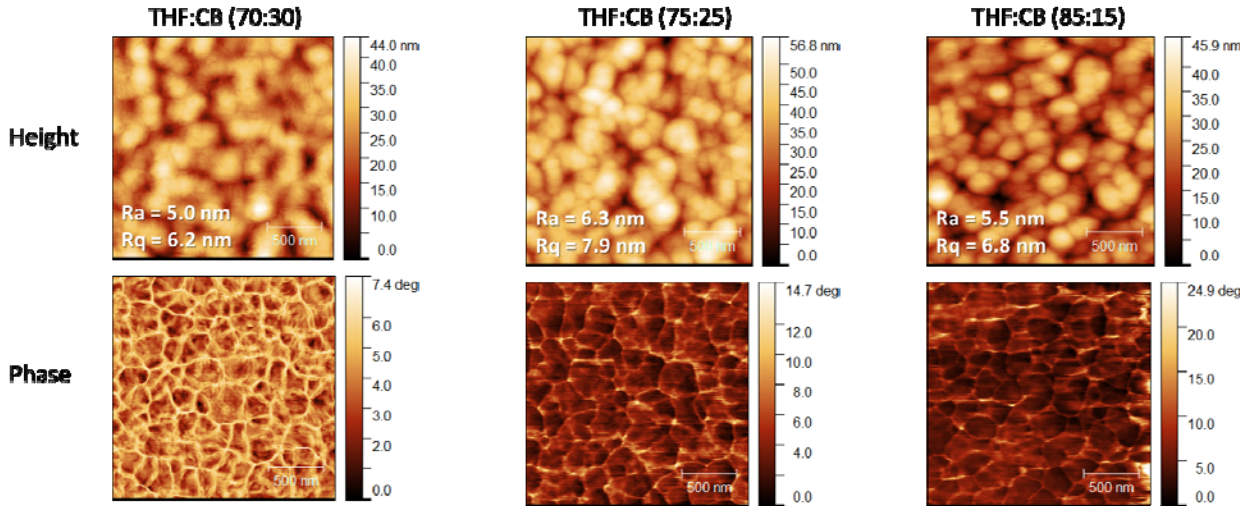

Fig. 11. AFM height and phase images of RCN_4T_B:$PC_{71}BM$ films prepared with different co-solvent ratios.

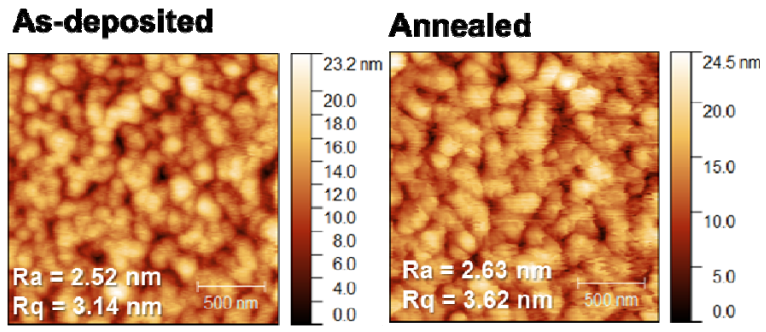

Fig. 12. AFM height images of as-deposited and thermally annealed RCN_4T_B:$PC_{71}BM$ films.

We discovered that how the solution containing both the HB-enabled donor and fullerene acceptor (PCBM) is prepared actually has a strong influence on the structural and photovoltaic properties of the blended film. Two different methods were used to prepare such solutions: directly mixed (DM) and separated mixed (SM). The DM solution (as we have used from the very beginning) was prepared by dissolving both the

HB donor and the fullerene acceptor in the same solvent (THF:chlorobenzene) together at a predetermined ratio. The SM solution was prepared by first dissolving the HB donor in THF and the fullerene acceptor in chlorobenzene separately (with stirring) followed by mixing the donor:THF and acceptor:CB solutions at a predetermined ratio. The SM solution preparation method allowed better solvation of the HB-enabled donor species than the DM solution preparation method, hence the former yielded a better mixing of the donor and acceptor species in the films than the latter. As shown in Fig. 13, only ~50% suppression in the photoluminescence (PL) from the RCN_4T_B donor molecules was obtained in the donor:acceptor mixed films prepared using the DM method. The PL quenching was improved to ~70% when the mixed film was prepared using the SM method.

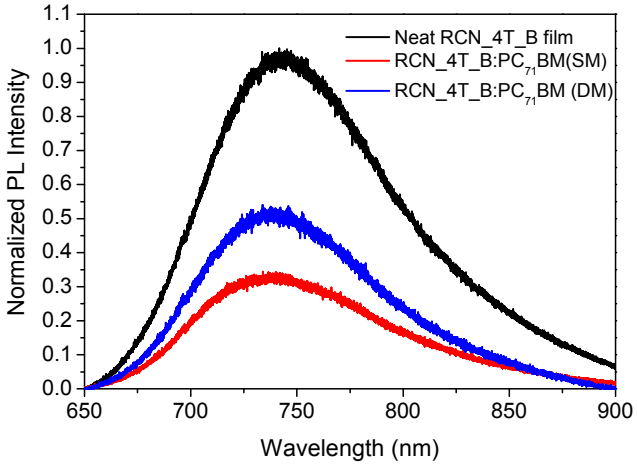

Fig. 13. PL spectra of neat RCN_4T_B film and RCN_4T_B:PCBM films prepared using DM and SM methods.

The SM solution preparation method also helped us to achieve less phase separation in the HB-enabled donor:fullerene blends. As shown in Fig. 14, the as-prepared RCN_4T_B:PCBM film (the HB blend film) has domain sizes as low as 20 nm, while the RCN_4T_BMe:PCBM film (the comparator blend film) has domains with typical size >60 nm. The HB blend film also is significantly smoother than the comparator blend film (r.m.s. roughness: 1.4 nm vs. 3.0 nm). Upon annealing at 140°C, both films appear to show stronger degrees of molecular aggregation, as shown in Fig. 15. The domains become more fiber-like and elongated. Nevertheless, it is still clear that the HB blended film still possess much finer domains than the comparator (Me) blended film.

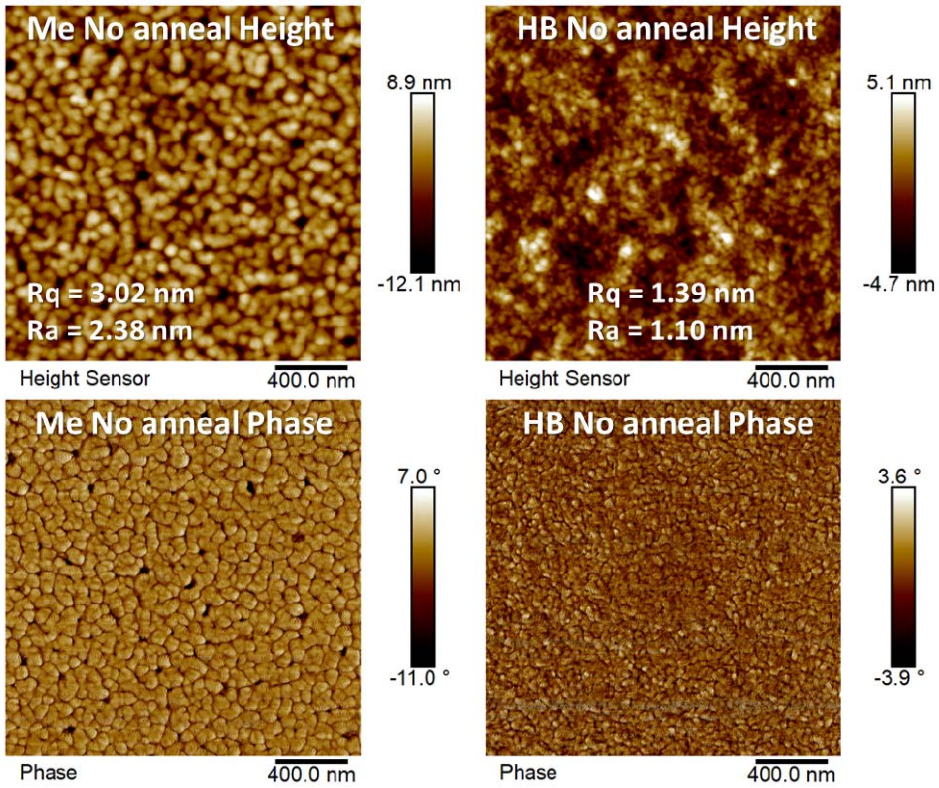

Fig. 14. The AFM height (upper row) and phase (lower row) images of as-prepared (i.e., no annealing) RCN_4T_B:PCBM film (the HB blend film, right column) and RCN_4T_BMe:PCBM film (the comparator Me blend film, left column)

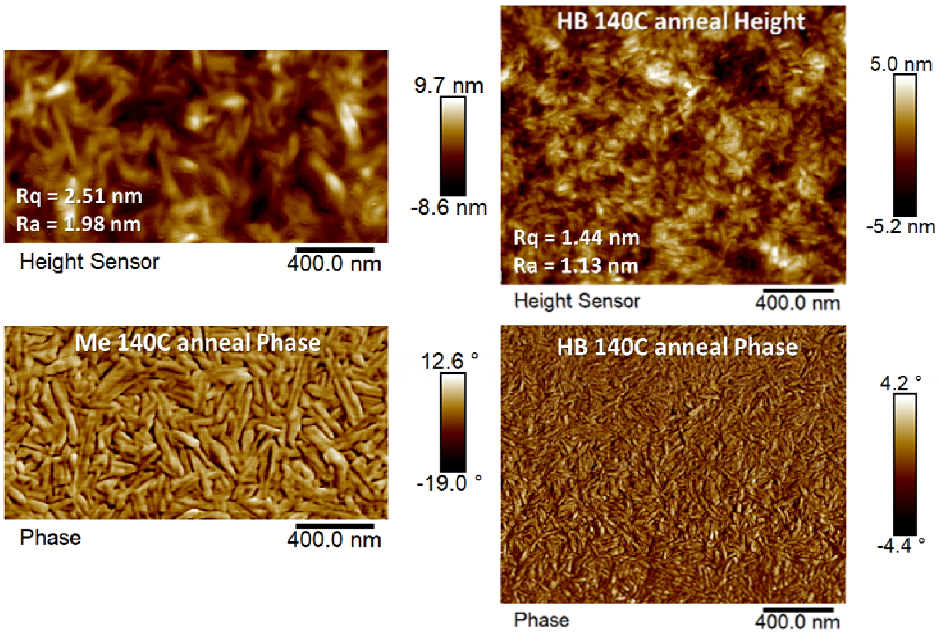

Fig. 15. AFM height (upper row) and phase (lower row) of RCN_4T_B:PCBM film (the HB blend film, right column) and RCN_4T_BMe:PCBM film (the comparator Me blend film, left column) after annealing at 140°C

We used X-ray diffraction (XRD) to help us understand the crystallinity and molecular orientation of the neat and blended films. As shown in Fig. 16, the as-cast HB neat film exhibits greater crystallinity than the comparator film. For both blended and neat films, RCN_4T_B becomes more crystalline with annealing. In contrast, it appears that PCBM breaks up the packing structure for the blended comparator film. Both RCN_4T_B and RCN_4T_BMe molecules appear to have some preferred edge-on oriented packing structures, although this does not preclude the possible existence of face-on oriented stacks due to the geometry of the XRD experiments performed here. We will use grazing-incidence wide-angle X-ray scattering (GIWAXS) to fully determine the orientation of the molecular stacks.

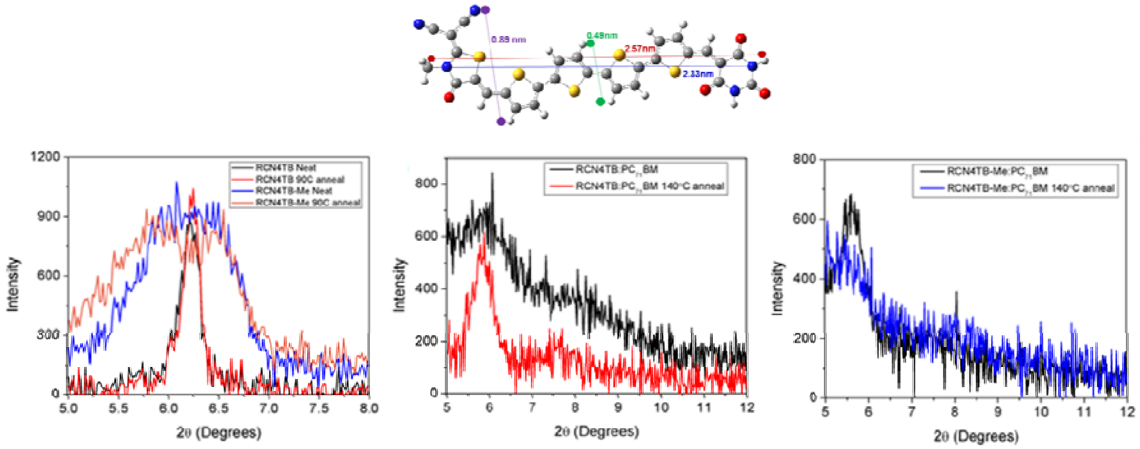

Fig. 16. X-ray diffraction patterns of as-casted and annealed neat RCN_4T_B and RCN_4T_BMe films (left), RCN_4T_B:PCBM (middle), and RCN_4T_BMe:PCBM (right) films

5. Fabrication, characterization, and optimization of organic solar cells

Using the synthesized new HB-D oligomers and the comparator RCN_5T_RCN, we have fabricated organic solar cells using the general structure of ITO/PEDOT:PSS/active layer/Al, in which the active layer consisted of 1:1 mixed (by weight) donor oligomer and fullerene (either $PC_{61}BM$ or $PC_{71}BM$) mixtures.

For the comparator molecule RCN_5T_RCN mixed with $PC_{61}BM$, we obtained a PCE of 1.2% in the solar cell with no post-deposition thermal annealing. The PCE was increased to 1.9% after 10 min annealing at 90°C, and further to 2.3% after 10 min annealing at 120°C (see Fig. 17). From the EQE spectra, we observed a near doubling in EQE when a -4 V reverse bias was applied. This suggests some charge extraction issues in these devices, which was also evidenced from the relatively low fill factor of the solar cells (FF ≤ 0.50). The literature report on DRCN5T achieved a highest efficiency of ~10%, using $PC_{71}BM$ as the acceptor and a PFN interlayer at the active layer/cathode interface for improved charge extraction. So clearly some improvements can be made on our benchmarking devices.

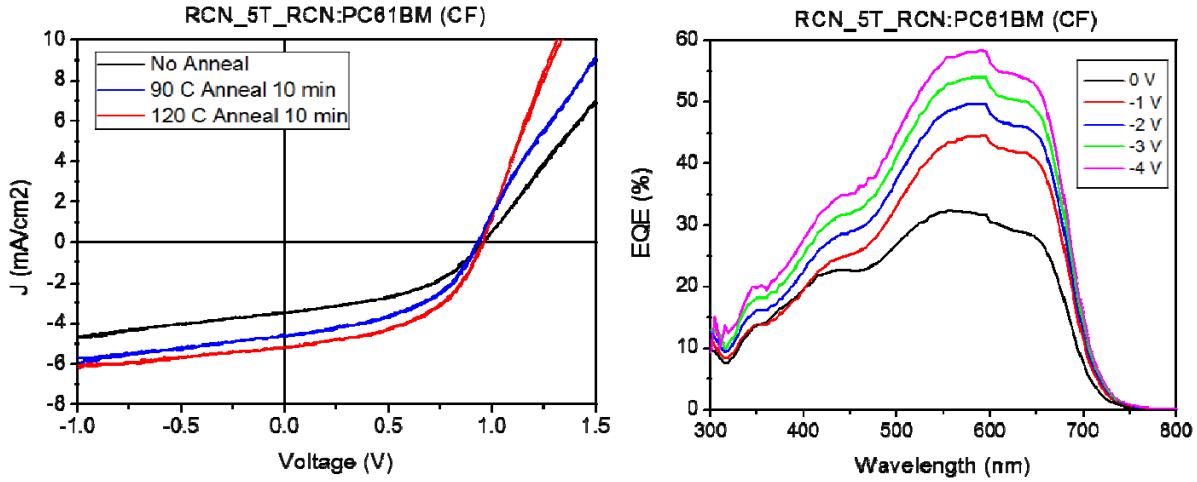

Fig. 17. (left) Current density-voltage (J-V) characteristics under simulated 1 sun AM1.5G illumination for RCN_5T_RCN:$PC_{61}BM$ organic solar cells with no post-deposition thermal annealing or 10 min thermal annealing at 90°C or 120°C; (right) EQE spectra under short-circuit (0 V) or various reverse biases of a representative RCN_5T_RCN:$PC_{61}BM$ organic solar cell.

We compared the performance of RCN_4T_B:$PC_{71}BM$ solar cells using the DM or SM method to prepare the mixed solution. As shown in Fig. 18a, The SM device show improved short-circuit current (4.8 mA/cm^2 vs. 3.4 mA/cm^2) and fill factor (37% vs. 34%) over the DM device. The PCE of the SM device reached 1.8% (best device 1.95%), as compared to 1.2% for the DM device. Thermal annealing does not results in improvement in PCE of these solar cells; instead, the efficiency is decreased to 1.5-1.4% with 80-110°C annealing due to the reduction in the external quantum efficiency (Fig. 18b). It is worth noting that a high open-circuit voltage of 1.05 V was obtained from these devices, which is very high for organic solar cells with light absorption above 700 nm.

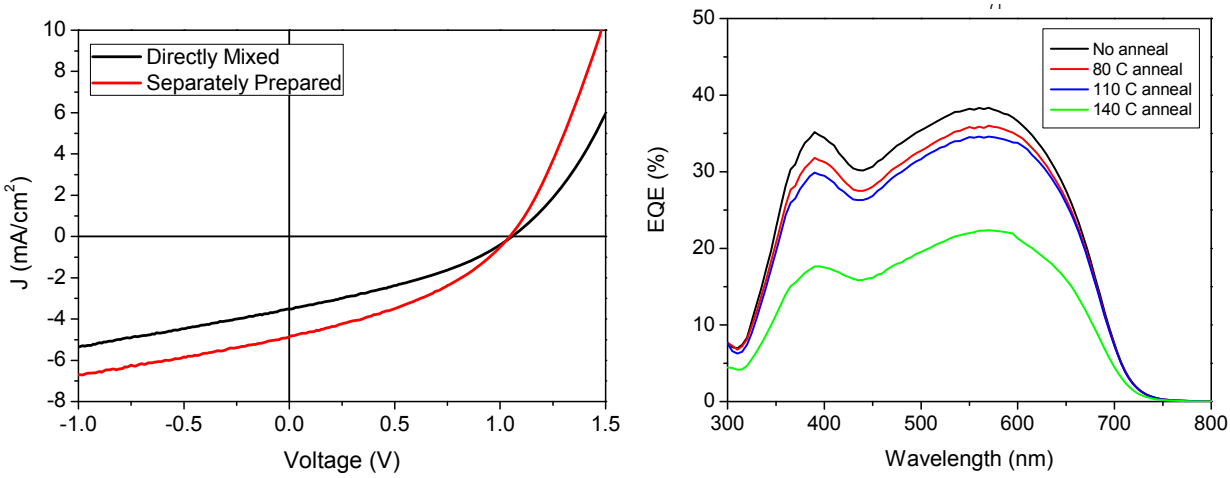

Fig. 18. (a) Current density-voltage (J-V) characteristics of RCN_4T_B:$PC_{71}BM$ solar cells under simulated 1 sun AM1.5G illumination with the blended film prepared from

directly mixed (DM) or separately mixed (SM) solutions. (b) External quantum efficiency (EQE) spectra of the SM RCN_4T_B:$PC_{71}BM$ solar cells upon annealing the devices at various temperatures.

As shown in Fig. 19a, the HB-enabled molecules show significantly higher photovoltaic performance in the resulted solar cells than the corresponding HB-disabled (Me) comparator molecules. For both unannealed devices, the PCE of the HB device is 2.6 times that of the Me device, primarily due to the higher photocurrent response. The optical absorption properties of the HB and Me films are, however, almost identical as shown in Fig. 19b.

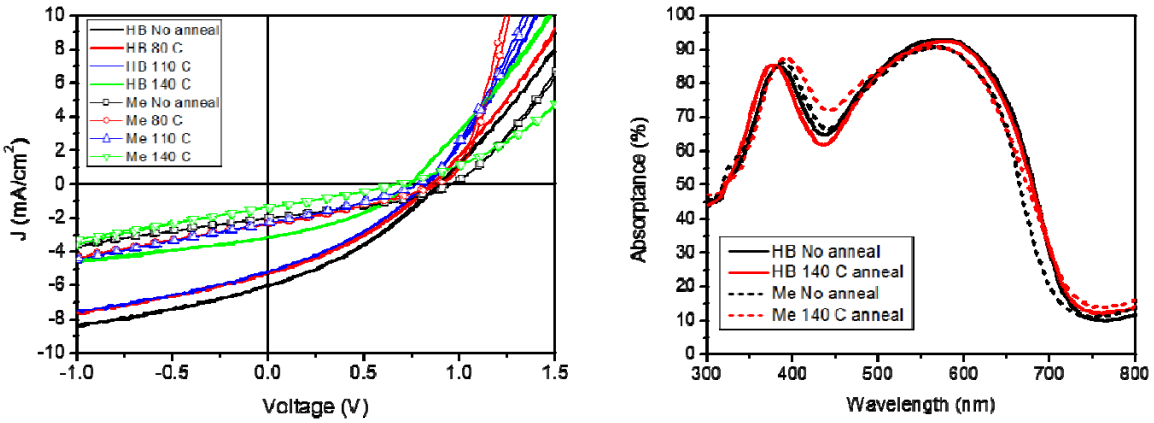

Fig. 19. (a) Current density-voltage (J-V) characteristics of RCN_4T_B:$PC_{71}BM$ (HB-enabled) and RCN_4T_BMe:$PC_{71}BM$ (HB-disabled, Me) solar cells under simulated 1 sun AM1.5G illumination. (b) Absorption spectra of the as-cast (no anneal) and annealed HB and Me blended films.

The DFT calculations predicted that RCN_5T_B should have even longer wavelength absorption than RCN_4T_B due to the longer thiophene oligomer used. Initial attempts to make solar cells with RCN_5T_B:$PC_{61}BM$ active layers have not resulted in good photovoltaic performance. Fig. 20a shows the J-V characteristics of three RCN_5T_B:PCBM solar cells with the blended film casted from THF:CB (4:1) so-solvent, which resulted in 90-100 nm thick blended films. A maximum PCE of 0.73% was obtained, with the external quantum efficiency peaked at about 20%. By examining the film absorbance (Fig. 20b), we discovered that the blended films do not contain much RCN_5T_B, which is likely due to the relatively low solubility of RCN_5T_B in the THF:CB (4:1) co-solvent.

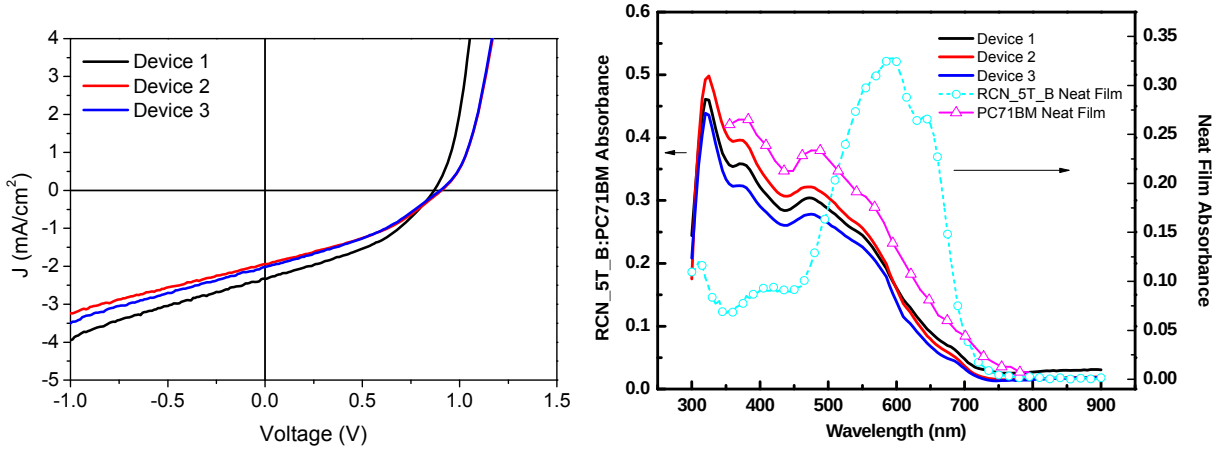

Fig. 20. (a) Current density-voltage (J-V) characteristics of three RCN_5T_B:$PC_{71}BM$ solar cells under simulated 1 sun AM1.5G illumination. (b) Absorption spectra of the RCN_5T_B:$PC_{71}BM$ blended films as compared to that of the neat RCN_5T_B film.

Comparison of Actual Accomplishments with Project Objectives:

Through this SIPS project, the UF research team designed and synthesized a series of new low-band-gap organic donor oligomers with integrated hydrogen-bonding functionality, and applied them to fabricate bulk heterojunction organic solar cells. These new donor oligomers rely on the commonly adopted donor-acceptor structure to lower the band gap, thus extending the absorption to longer wavelength portions of the solar spectrum. The covalently coupled HB moiety, on the other hand, directs the supramolecular assembly of these A-D-HB oligomers into particular architectures (trimers, hexamers, etc.). Using the general structure of RCN_nT_B (where B=barbiturate, and n = 4,5), we achieved light absorption above 700 nm and a high open-circuit voltage exceeding 1 V in the resulted bulk heterojunction solar cells. The power conversion efficiency of the solar cells containing the HB-enabled oligomers is 2.6 times that for the HB-disabled oligomers, which is consistent with what we have observed previously for quaterthiophene-based devices. This re-confirms the positive impact of the HB unit in our donor oligomer design on (supra)molecular assembly and bulk heterojunction morphology. However, the highest efficiency we have obtained for the organic solar cells is significantly lower than the original anticipated efficiency (15%).

We have also faced new challenges, specifically in the purification and solution processing of these HB-containing oligomers, which we only partially addressed through the course of this project. To fully dissolve these oligomers together with fullerene, we had to use a co-solvent system in which one component is HB-compatible (for dissolving the HB oligomer) and the other is a good solvent for fullerene. This presented a multitude of complications for material processing, some of which were successfully addressed such as impact of moisture content in THF and direct vs. separate mixing of the blended solutions. However, ultimately we did not have sufficient time to perform multiple iterations on the oligomer design, particularly on alkyl chain attachment (number of alkyl chains on each oligomer, location, length, etc.), which strongly

influences the solubility in common solvents (chloroform, chlorobenzene, etc.) that are used for fullerene.

Another challenge in this work is the inconclusive determination of the orientation and stacking of the HB-functionalized donor oligomers. Previously in our study of vacuum-deposited quaterthiophene based oligomers (with phthalhydrazide as the HB unit), we observed in-plane HB-interaction and out-of-plane π-stacking, meaning the oligomers adopted a "face-on" orientation on substrate. However, in the solution processed RCN_4T_B:PCBM films studied in this project, we did not obtain the same type of molecular organization in the solid state. It may be due to the six-fold HB interaction for barbiturate units, which may be more difficult to form than the trimers for the phthalhydrazide units as six molecules will have to act together instead of three. On the other hand, we also hypothesize that the solution processing environment may also make it difficult to form vertically oriented π-stacks; a long stack may have a preferential in-plane orientation due to its aspect ratio (>50 nm in length and <5 nm in diameter). This could explain why we observed elongated domains in the annealed films. The situation could be a bit different in vacuum deposition as molecules arrive on the surface continuously, instead of being all present at once as in the case of solution processing. Thus, vacuum deposition may give HB-oligomers time to organize into trimers/hexamers through hydrogen bonding. The interaction of the molecules with the substrate surface and molecules already on surface may also provide the necessary environment for the oligomers to orient "face-on". Considering these possibilities, we started the synthesis of phthalhydazide terminated low-gap oligomers that may be vacuum processible, an example of which is RCN_3T_PH (shown below). Unfortunately, the last step conversion in synthesizing this compound is unexpectedly complicated. The RCN-3T unit apparently caused several different conversion methods to fail even though they all worked when RCN-3T is not present. Alternative methods were developed, however, they were not completed when the project ended.

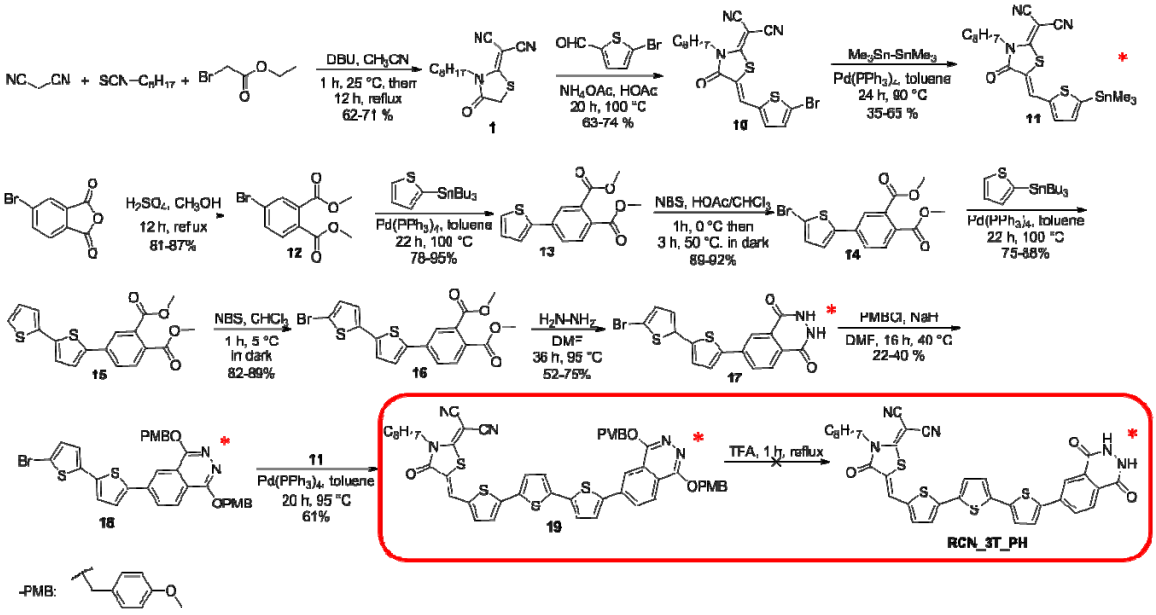

Products Developed Under the Award:

a. Publications (list journal name, volume, issue), conference papers, or other public releases of results.

Journal papers:

A. O. Weldeab, A. Steen, D. J. Starkenburg, J. S. D. Williams, K. A. Abboud, J. Xue, N. I. Hammer, R. K, Castellano, and D. L. Watkins, "Tuning the structural and spectroscopic properties of donor-acceptor-donor oligomers via mutual X-bonding, H-bonding, and π-π interactions", *J. Mater. Chem. C* 2018 (doi: 10.1039/C8TC00074C).

Daken J. Starkenburg, Asmerom O. Weldeab, Lei Li, Zhengtao Xu, Danielle E. Fagnani, Xiaoyang Yan, Xueying Zhao, Michael J. Sexton, Scott S. Perry, Ronald K. Castellano, and Jiangeng Xue, "Self-assembly of a hydrogen bonding oligothiophene derivative with donor-acceptor molecular design to enhance organic solar cell performance", to be submitted.

X. Zhao, D. J. Starkenburg, A. O. Weldeab, D. E. Fagnani, J. Xue, R. K. Castellano, and S. S. Perry, "Hydrogen bonding mediated self-assembly of functionalized bithiophenes on Au surfaces", to be submitted.

Conference papers:
R. Castellano, J. Xue, and S. Perry, "Hydrogen Bond Directed Self-Assembly of Molecular Donors for Organic Photovoltaics", 2017 Materials Research Society Spring Meeting, April 17-21, 2017, Phoenix AZ

Asmerom Weldeab, Daken Starkenburg, Danielle Fagnani, Lei Li, Zhengtao Xu, Scott Perry, Ronald K Castellano, and Jiangeng Xue, "Hydrogen Bond Directed Self-Assembly of Molecular Donors for Organic Photovoltaics", 2018 Materials Research Society Spring Meeting, April 2-6, 2018, Phoenix AZ

Dissertation and Theses: Results from this project have been incorporated into three doctoral dissertations at University of Florida

Asmerom O. Weldeab, Ph.D., Chemistry, December 2017
Danielle E. Fagnani, Ph.D., Chemistry, May 2018
Daken J. Starkenburg, Ph.D., Materials Science and Engineering, August 2018 (expected)

b. Web site or other Internet sites that reflect the results of this project;

None.

c. Networks or collaborations fostered;

Developed collaboration with CHESS (Cornell University) on x-ray scattering characterization of organic thin film morphologies

d. Technologies/Techniques;

The University of Florida has previously patented the hydrogen-bonding-mediated supramolecular self-assembly approach to organic bulk heterojunction photovoltaic devices. This project contributed to the further development of this technology by expanding the photoactive materials to longer-wavelength solar spectral coverage and solution processing for thin-film deposition.

e. Inventions/Patent Applications, licensing agreements; and

None.

f. Other products, such as data or databases, physical collections, audio or video, software or netware, models, educational aid or curricula, instruments or equipment.

None.